Effect of polymeric architecture on anisotropic soft matter

A Synopsis of the Thesis to be submitted to the Mangalore University

for the Award of the Degree of Doctor of Philosophy in Physics

Submitted by

Marlin Baral
Senior Research Fellow
Registration No- MU/EXB/Ph.D./CR.65/Phy./2018-19/E.13
Enrolment number-166181705
Centre for Nano and Soft Matter Sciences (CeNS)
Bengaluru-56001

Under the Supervision of

Dr. S. Krishna Prasad

Centre for Nano and Soft Matter Sciences (CeNS),
Prof. U. R. Rao Road, P. B. No. 1329,
Jalahalli, Bangalore – 560013.

October 2020

SYNOPSIS

Name of the student: Marlin Baral,
Senior Research Fellow,
Centre for Nano and Soft Matter Sciences (CeNS),
P.O.Box No.1329, Jalahalli,
BANGALORE – 560013

Name of the Supervisor: Dr. S. Krishna Prasad,
Honorary Professor,
Centre for Nano and Soft Matter Sciences (CeNS),
P.O.Box No.1329, Jalahalli,
BANGALORE – 560013

Thesis title: **Effect of polymeric architecture on anisotropic soft matter**

Registration No: MU/EXB/Ph.D./CR.65/Phy./2018-19/E.13 dated 18.02.2017

Introduction

Liquid crystals, also referred to as mesophases, are thermodynamically stable phases of matter generally observed between the three-dimensionally ordered crystalline solid and the highly disordered isotropic liquid [1-2]. A liquid crystal (LC) phase is unique in its properties, because it flows like a liquid but at the same time shows anisotropic physical properties which is a characteristic of solid. The basic geometrical form of the molecules giving rise to liquid crystallinity is mostly a rod or a disk like, which allow close, quasiparallel packing. Transition to this intermediate state can be brought about either by the influence of temperature (themotropic mesomorphism) or by the influence of the solvents (lyotropic mesomorphism). Apart from the fundamental interest, LCs have attracted attention owing to the reorientation of the molecule and the associated fast electro optic response caused by the application of low voltages resulting in LC devices that dominate the flat panel as well as flexible display technology [3].

Historically thermotropic LC phases of rod shaped molecules are mainly classified into three categories viz., nematic, cholesteric and smectic. In the nematic phase, the molecules posses only a long range orientational order, but no positional order; the preferred axis of the spontaneous orientation is denoted as the director, **n**. The cholesteric or chiral nematic phase exhibited by optically active molecules, is essentially a nematic phase except for a superimposed helical axis normal to the director. In a smectic phase the centre of gravity of molecules are arranged in equidistant layers creating a one dimensional positional order in addition to the orientational order. The subtle interplay between the different types of order and the structure yields as many as 40 different LC phases. Apart from these classical phases, the relatively young class of bent-core or banana-shaped LC materials exhibit eight well established phases, labelled simply B1 to B8 [4]. Owing to their special shape, the bent-core molecules favour packing into lamellar structures with a tendency to exhibit the attractive in-plane polar order.

Devices based on confinement of nematic liquid crystals (NLCs) in a polymeric matrix have huge potential for use in spatial light modulation and electrically controlled transparency applications. The principle involved is the nano-level phase separation of two specifically chosen soft materials (liquid crystal and a polymer) with tailor-made refractive index values. The situation is similar to the atmospheric fog wherein the two materials – water droplets and air –

satisfy similar conditions. An applied electric field chooses between the two situations, of matching or mis-matched indices between the polymer and liquid crystal. This electric effect results in an optical output, which at the flip of a switch, alters between scattering and transparent states of the device. Encapsulation of this active material between glass sheets or flexible substrates leads to smart switchable windows which have a wide range of possible applications spanning household, healthcare, privacy creation, smart displays and energy saving domains. [5-12] This thesis discusses the effect of polymeric architecture on the various liquid crystals such as liquid crystals doped with certain nano-particles and organic emitters. The thesis contains seven chapters, with Chapter 1 providing the required introduction to the liquid crystal phases and phase sequences along with a description about the various kinds of polymerization processes to create polymer stabilised (PSLCs) and polymer dispersed (PDLCs) liquid crystal architecture. The next six chapters can be divided into three sections, section 1 comprising Chapter 2 and 3 describes the reinforcement of the polymer architecture by carbon nanoforms (such as, CNTs and graphene) and the consequence influence on the electro-optical properties of PSLC device. Section 2 that includes chapter 4, 5 & 6 brings out the enhancement of PL from an organic emitter while being in an LC environment specifically through Chapter 4 describes the enhancement of the PL realized via a novel wavelength matching technique between the photonic band gap (PBG) of the cholesteric and the excitation wavelength of the incorporated organic fluorophores. Based on this concept, it also leads significant PL anisotropy to a further enhancement of PL and a three state fluorescent memory device are delineated in chapter 5 highlighting the importance of polymer stabilization in a cholesteric- fluorophore system. Chapter 6, introduces the concept of conjunctive pathway of the aforementioned wavelength matching technique and the metal enhanced fluorescence to drastically increase PL, way beyond a mere arithmetic addition of the value realized through each of the separate pathways. Additional advantage of the conjunctive pathway is seen in the dissymmetry factor characterising chiral discrimination measured using circular polarised luminescence. The last chapter on results, Chapter 7 discusses the effect of polymer stabilization on the thermal and dielectric characters of an antiferroelectric liquid crystals. Chapter 8 provides an overview of the results presented and an outlook for future developments. A chapter-wise summary of the prominent aspects dealt in the thesis is given below.

Chapter 1: Introduction to liquid crystals

This chapter provides a brief introduction to the structure and classification of liquid crystals with emphasis on thermotropic liquid crystals that can be switched in an analog fashion with an electric field. The orientational order parameter, curvature elasticity, anisotropic material properties, ferroelectricity and viscosity coefficients are also discussed. It also describes the two main types of liquid crystal polymer composites, viz., polymer stabilized liquid crystal (PSLC) and polymer dispersed liquid crystal (PDLC).

Chapter 2: Carbon nanotube reinforced polymer stabilized liquid crystal device: Lowered and thermally invariant threshold with accelerated dynamics

This chapter describes the effect of reinforcing a polymer stabilized network on the electro-optic and dielectric properties of the confined liquid crystal system.. The known aspect that the fibrils of the polymer provide the virtual *surfaces* with finite anchoring energy leading attractive electro-optic properties is further improved by the novel route of mechanical reinforcement of the fibrils. The studies aim at achieving a sturdier polymer network without increasing the polymer concentration. The concept used is akin to strengthening concrete by reinforcing it with steel rods. This novel variation of the PSLC device is achieved by reinforcing the main polymer fibrils with polymer-capped single-walled carbon nanotubes (CNTs). The amelioration is caused by the grafting of the polymer in to the CNTs and thus is structurally identical to that of the matrix. This results in good compatibility between CNTs and the matrix prevents the CNTs from drifting away from the matrix polymer, which is a limitation in the previous attempts to have CNTs in PSLC systems. Difference in the morphology of the polymer strands observed is proposed to be indicative of the increased mechanical strength by the incorporation of the CNTs. The most interesting feature of the PMMA-CNT system was its thermal behaviour of Vth. Figure 1 represents the temperature dependence of the threshold voltage for both the PMMA-CNT and PMMA-b (no- CNT material) system which covers the useful operating thermal range. There is a notable difference in both the profiles. For the PMMA-b there is a monotonous decrease in the threshold voltage with the increase in the temperature which is a typical of

nematic material. However, in contrast, the mixture incorporating PMMA strands tethered to CNT leads to, an essential temperature independence of Vth even at the small concentration used. Besides, the magnitude of the threshold voltage is reduced and the switching dynamics accelerated. This feature is very crucial from device point of view as it reduces the complexity of the driving circuitry.

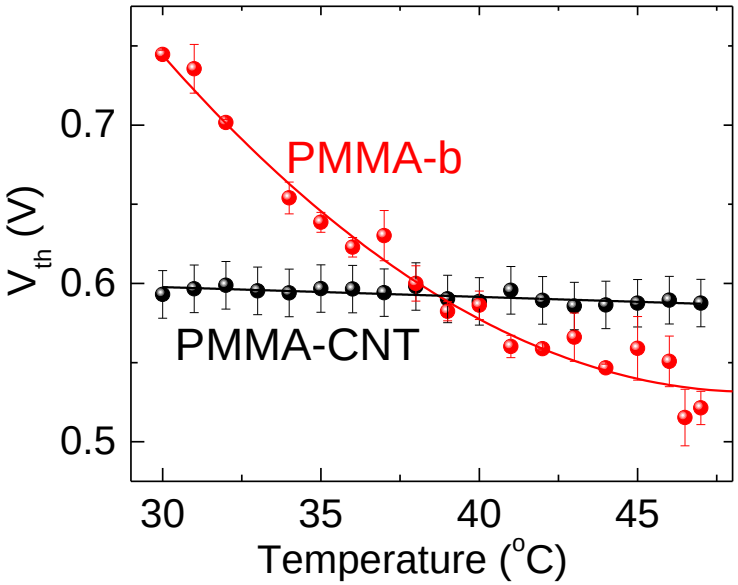

Figure 1: Thermal dependence of the threshold voltage for the two polymer stabilized samples presenting a striking difference between the two. While PMMA-b exhibits a sizeable increase on lowering the temperature, behaviour typical of nematics, including polymer stabilized ones, for the SWCNTs-reinforced PMMA V_{th} is essentially independent of temperature.

Chapter 3: Graphene augmented polymer stabilization: Drastically reduced and temperature independent threshold and improved contrast liquid crystal device

This chapter discusses about the employment of the graphene-LC in the polymer network. The system being termed PSGLC. Comparisons are made between the host PSLC (without any graphene) and the PSGLC systems in terms of the morphology (as imaged by SEM) and electro-optic characteristics. The PSGLC does exhibit a characteristically different morphology and more importantly, markedly enhanced electro-optic features: Substantially lowered threshold voltage, thermally invariant threshold and dynamic switching without backflow; each of these is highly desirable and brings out the importance of graphene in the medium. A feature that contrast the present study with the previous ones (e.g., Ref. 16) is the realization that certain

enhancements of the properties, such as the lowering of the threshold, can be achieved by working at very low concentrations of the filler material. A further novelty that we highlight here is the powerful template technique: Create the necessary polymer architecture with the required mechanical strength and alignment, leech out the host and introduce the desired operating material. With this protocol the strengthening can be done with one set of host nanocomposites while deploying another optimized host material for the device operation. Thus, the present studies bring in a generalization to the concept of achieving drastically improved PSLC systems by keeping the polymer content low but concomitantly make the polymer fibers mechanically stronger. The generalization serves in two ways: (i) any nano-soft composite can be used as the host and (ii) the electrical characteristics of the nanostructure in the template creating host do not limit the operation of the device. Combined with the expected enhanced mechanical strength, these observations signify a novel approach to have a robust PSLC system using minute quantities of carbon nanoforms.

Depending on the concentration of the polymer content, they are divided into two types: Polymer dispersed liquid crystals (PDLC) where in the polymer content is higher than that of the liquid crystal, and polymer stabilized liquid crystals (PSLC) in which polymer is the minority component. Owing to the larger polymer content, PDLCs have higher mechanical strength and thus, are less prone to damage due to mechanical shocks. But the threshold voltage i.e., the minimum operating voltage for the device to switch from the transparent ON state to the scattering off state is high, due to large number of polymer strands which increase the anchoring strength of the system. But for PSLC, due to lower polymer content the threshold voltage is lower than that of PDLC but it is not as robust as PDLCs due to the lower concentration of polymer. Thus the challenge is to strengthen the polymer part without adversely affecting the operating voltage. Obvious candidates for the purpose are nanoparticles of appropriate kind. In point of fact, substantial attempts [13-15] have been done in investigating the influence of nanoparticles on LC properties, and effects, including reduction in the threshold voltage, are observed in such nanocomposites. However, with hardly any exception, these efforts are based on pure liquid crystal composites and not on any polymeric system. [16] It may be mentioned that a combination of PSLC-in-PDLC had been reported to achieve the dual requirement of mechanical strength, but lower operating voltage. It is notable that to achieve this, the authors employed three different polymerizable monomers, a complex system indeed: while two

polymers provided the droplet morphology, the third one gave the PSLC architecture. However, the drastic reduction in the threshold voltage, a parameter that is of fundamental importance from the device perspective, is seldom seen. More importantly, none of these papers reported the temperature invariance of the threshold voltage, a parameter that certainly simplifies device driver fabrication. In contrast, the work discussed in this and the previous chapter not only achieves the same effect with just one monomer and a very small concentration of carbon nanoforms, but presents important features also.

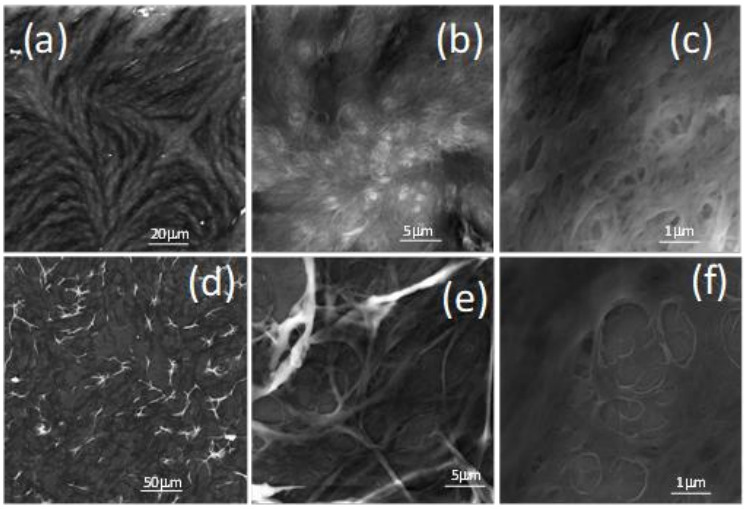

Figure 2: SEM images of the PSLC (a-c) and PSGLC (d-f) after removing the contained host liquid crystal and also removing the top plate from the cell. The morphological differences between the two cases are more evident in panels b and e.

The Field emission scanning electron microscopy was carried out by washing out the LC and opening the cells. FESEM images are shown in Figure 2(a-c) for PSLC and d-f for PSGLC. The morphology in the two cases is clearly seen to be quite different. The PSLC has a strong tendency to form bundles of sizeable thickness (Figure 2b) where as PSGLC has thinner strands (Figure 2e). This leads to the fact that keeping the same polymer content can lead to a larger surface area offered by the polymer fibres. Since virtual surfaces provided by the polymer fibres are associated with the PSLC, it is always advantageous to have a large number of thinner fibres. The focus of the PSLC is not uniform over the imaging area even on the linear dimensions of 30□m (figure 2a and b). Whereas the focus of the PSGLC is always sharp. We argue the reason for this is that the out of plane transverse is much less in the case of PSGLC. A point to be noted here that the PSGLC mimics the droplet or Swiss-cheese morphology. This indicates that the

presence of graphene as a nano-filler makes the polymer fibres very strong in case of PSGLC. It is well known that the different carbonaceous forms when used as nano fillers in the polymeric materials result in significant improvement in the mechanical strength of the polymer. In order to get an evidence for the presence of graphene in the polymer matrix we carried out Raman spectroscopy measurements on PSGLC as well as the PSLC cells.

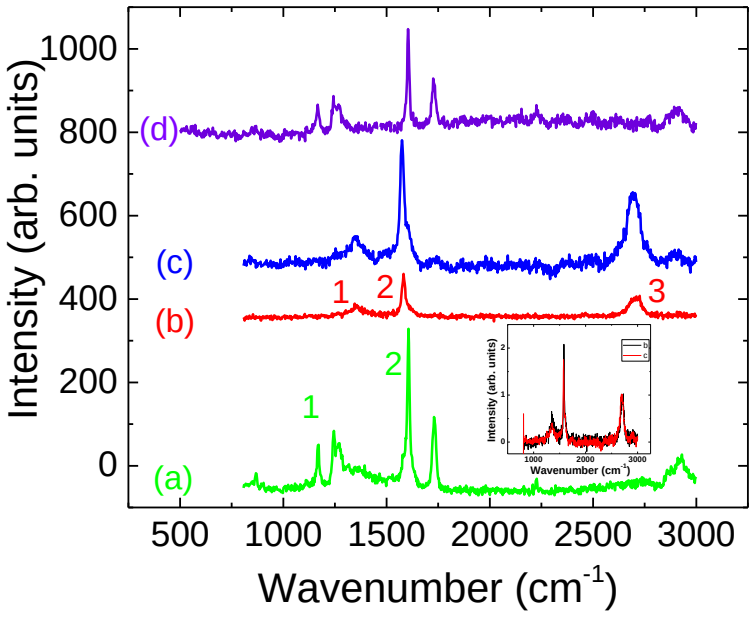

Figure 3: Sections of the Raman map depicted as "one-dimensional" Raman spectra of the PSLC (scan d) and PSGLC (scans a-c) systems. Scans (a) and (b) indicate polymer-dominant and graphene-dominant areas of the PSGLC film, whereas the scan (c) is from a region which contains both materials. For the scan (a) the peaks identified as 1 and 2 are from the C-C stretching in the biphenyl and phenyl moieties, respectively, as in fact found for PSLC (scan d). In (b) peaks 1-3 correspond to the D, G and G' bands of graphene, respectively. The inset shows that if the data is normalized with respect to the G' band intensity then the sets (b) and (c) are essentially identical

The exemplary Raman spectra over a larger wavenumber range are given in Figures 3 for the PSLC sample as well as at different spatial positions of the PSGLC film. Scans (a) and (b) indicate polymer-dominant and graphene-dominant areas of the PSGLC film respectively, whereas the scan (c) is from a region which contains both materials. For the scan (a) the peaks

identified as 1 and 2 are from the C-C stretching in the biphenyl and phenyl moieties, respectively, as in fact found for PSLC (scan d). In (b) peaks 1-3 correspond to the D, G and G' bands of graphene, respectively.

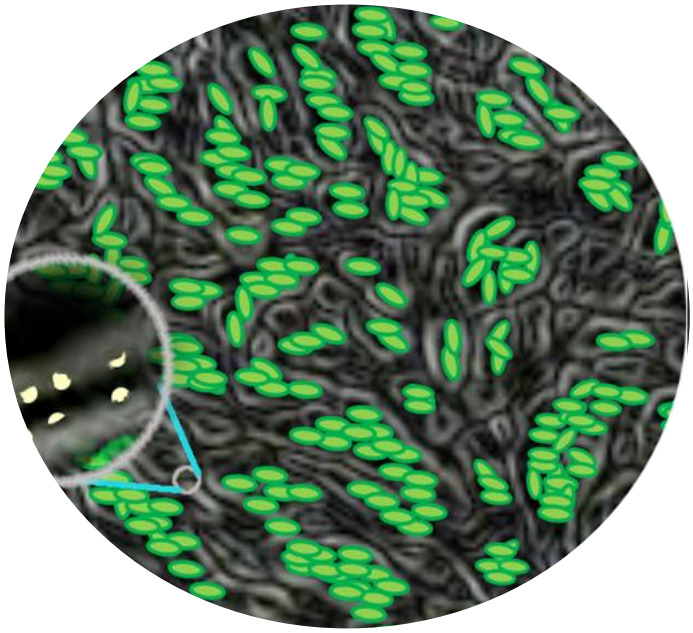

Figure 4: Schematic diagram illustrating the dispersion of the liquid crystalline molecules (green ellipses) in a polymer network (grey lines) strengthened by the presence of graphene flakes, which are proposed to be decorating the walls of the polymer fibres (especially in the template PSLC situation), as shown for an isolated fibre depicted in the blown-up inset.

In view of the information from microscopy and the Raman measurements described in this chapter it is proposed that the graphene incorporated polymer network would be like a "loofah" network with the graphene flakes decorating the surface of the fibres in spatially random way. This scenario is illustrated schematically in Figure 4 wherein the graphene decoration is highlighted in the inset of the illustration, a feature that is more realistic in the case of the template PSLC. The schematic diagram illustrates the dispersion of the liquid crystalline molecules (green ellipses) in a polymer network (grey lines) strengthened by the presence of graphene flakes.

Chapter 4: Giant Enhancement of Photoluminescence and Tertiary Emission in a Chiral Nematic by Matching Photonic Band Gap and Excitation Wavelength

This and the subsequent two chapters describe studies aimed at employing LC and polymer architecture to enhance PL of organic emitters with the ultimate goal of achieving emissive LCs for displays. The first of these, chapter 4, introduces a new concept that appeals to matching of two length scales and the associated light trapping mechanism. Photonic crystals (PCs) are periodic dielectric structures that can be employed to control and manipulate light propagation in a particular wavelength band which is referred to as the photonic bandgap (PBG). The cholesteric liquid crystals (CLCs) also exhibit one dimensional photonic band gap because of their spatial distribution of the refractive index. This chapter demonstrates that chiral nematic liquid crystal compositions incorporating fluorophores, wherein the photonic band gap (PBG) of the liquid crystal is matched with the excitation wavelength of the fluorophore results in (a) significant enhancement in the overall photoluminescence of the system and (b) eliciting secondary and tertiary emission such that a single low wavelength illumination can give emissions at multiple and highly desirable Red, Green and Blue wavelengths. The light-trapping strategy of matching the PBG with the excitation wavelength (λ_o), instead of the previously attempted protocol of matching with the emission wavelength (λ_{em1}), is shown to be superior in terms of the magnitude of emission and consequently, the quantum yield of the device. Further, it is shown that by using an applied electric field, three different emission levels can be achieved, two of them stable even when the field is switched off; the magnitude of the field provides a powerful handle to control the emission level with an overall change of a factor of 2. The three situations discussed here, no PBG, $\lambda_o \sim \lambda_{em1}$ and $\lambda_o \sim \lambda_{ex1}$ are schematically depicted in Figure 5.This clearly shows schematically that the extent of enhancement is maximum with the strategy of matching the excitation wavelength and the photonic band gap. The observed PL features are explained using radiative energy transfer mechanism and the short range ordering of the fluorophores, as obtained from X-ray diffraction experiments.

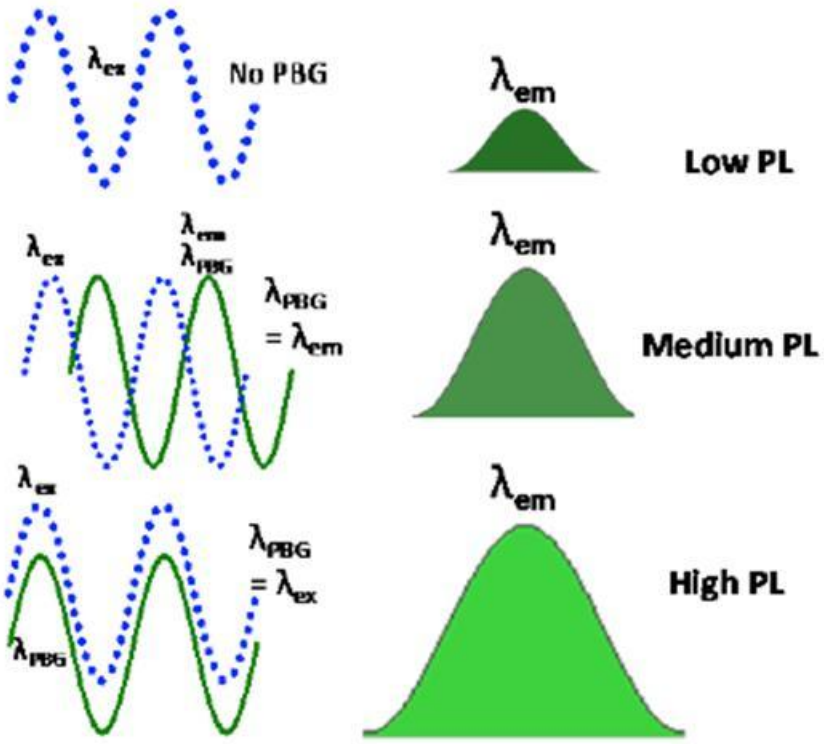

Figure 5: Schematic representation showing the three different scenarios of the wavelength matching concept (left) and the fluorescence output (right)

Chapter 5: Enhanced photoluminescence in a chiral nematic liquid crystal through polymer stabilization and an erasable 3-state memory device

Cholesteric liquid crystals can be switched among three states by applying different voltages. The application of a low voltage results in the focal conic texture (FCT) presenting a scattering appearance. The interesting aspect is that FCT is stable even after the removal of the field, creating a memory state that is created by applying a low voltage and subsequently removing it. Applying this concept and the concept of the novel wavelength matching which is described in chapter 4, an erasable memory device is proposed in this chapter which depicts three photoluminescence levels: the initial no voltage high PL, the low voltage intermediate PL and the high voltage, low PL. It also deals with confining a fluorophore comprising nematic in a polymer stabilized yielding to substantial (factor of ~ 3) enhancement of photoluminescence. This feature is found to be generic, applicable to non-chiral as well as chiral systems. However,

in the chiral systems presenting a photonic band gap (PBG), a second strategy of matching the helical pitch length with the excitation wavelength, further augments the emission yielding an overall gain factor of 16 between the native system and to one that has the network as well as PBG. Investigations as a function of the network density, defined in terms of the polymerizable monomer content X ranging over 0-6%, show that the emission level has a bell-shaped profile with X. It is further established that in each of these systems, an electric field reorienting the nematic molecules also alters the magnitude of photoluminescence. The effect, hardly seen for the no-network material and largest for the chiral system embedded in the network can act like a fluorescent photonic switch with less than 50 millisecond response. Analysis of X-ray diffraction and electron microscopy data bring out the importance of local ordering and morphology of the network.

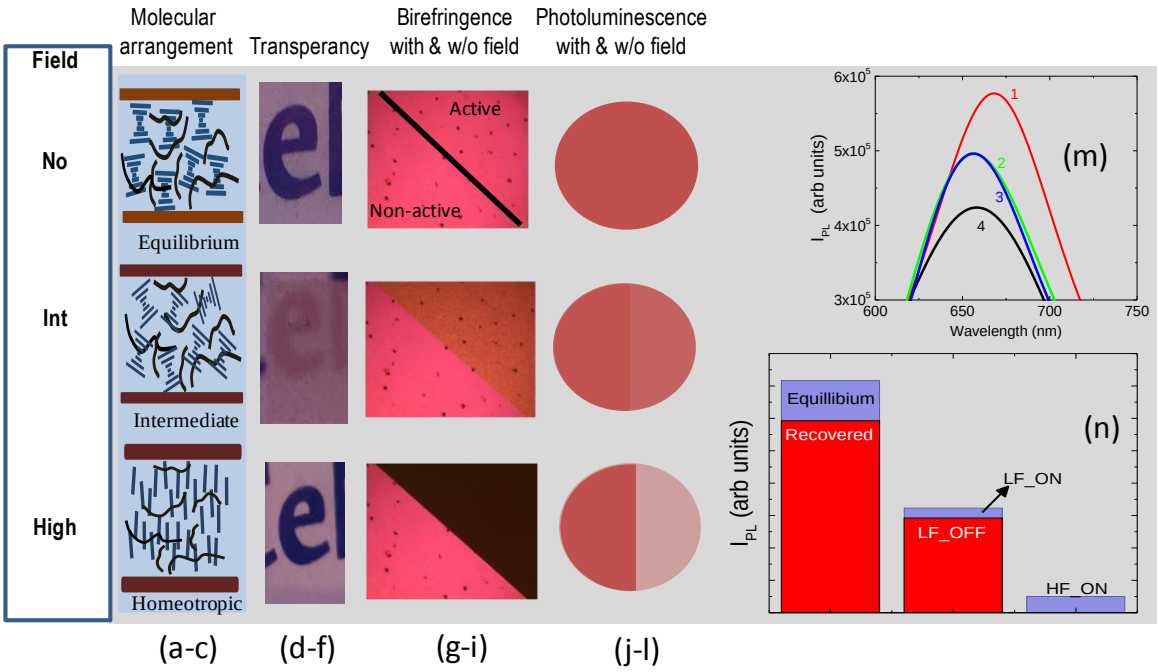

Figure 6: Composite diagram presenting the electric field-driven device under the no-field, intermediate field and high field situations.

In Figure 6, the panels (a)-(c) show the arrangement of the liquid crystal (or fluorophore) molecules and the polymer network. Panels (d)-(f) depicts that under equilibrium and high field conditions the device is transparent, but highly scattering for the intermediate field (e). This is illustrated here by viewing through the device text placed behind it. Birefringence contrast of the device for different field conditions with crossed polarizer configuration is shown in panels (g)-(i). For comparison, in each of these panels, the field-active (top-right) and non-active (bottom-

left) regions are shown. This influence is reflected in the magnitude of the emission also as represented in the panels (j)-(l). Again, the left-halves are from the non-active and the right-halves from the active regions. Panel (m) shows the emission spectra for the no-field (profile 1), intermediate field (profile 2) and high field (profile 4) exhibit substantial differences in the magnitude of PL. The memory effect of the emission is shown by the profiles 2 and 3 obtained immediately after applying the intermediate field, and some duration after switching it off. The essentially comparable profiles indicate long term memory. These features are more evident in the bar diagram (panel n) depicting the IPL values for the different states. The memory device can be operated in the high emission (equilibrium or completely recovered) state, or the intermediate PL value obtained by intermediate field or the low emission in the high field case.

Chapter 6: Conjunctive photoluminescence enhancement through plasmonic and photonic bandgap pathways in a chiral self-assembled system

Photoluminescence is currently a promising property for sensing applications owing to a variety of aspects including its simplicity, non-invasive, multi-analyte detection character.[17–20] There is an ever-increasing demand for enhancing the fluorescence without taking the parent emitter, e.g., the fluorophore, towards the undesirable photobleaching levels. Thus, the need of the hour is to retain the fluorophore intact and create structures externally which could interact with the fluorophores and increase the quantum yield for highly sensitive detection. A popular route is to appeal to the coupling the surface plasmon resonance (SPR) of the metal nanoparticles with the emitters, with the resulting feature referred to as the metal enhanced fluorescence (MEF) [21-23]. The increased electric field due to localized plasmon excitation helps to enhance the excitation rate of the dye molecules, although it is important to overcome the associated quenching. This chapter describes about two parallel pathways for enhancing the intrinsic photoluminescence of an organic emitter dispersed in a liquid crystal medium. The pathways have independent origins, arising from MEF and matching strategy described above. The former is realized by incorporating core-shell Gold nanoparticles, with the organic shell being made of pro-mesogenic cholesterol ester entities. A judicious combination of this pathway with the length scale PBG matching pathway achieves a level of photoluminescence which exceeds contribution due to the individual methods. This conjunctive protocol, schematically seen in Figure 7, results in an overall enhancement by a factor of 37 between the emitter dispersed in a non-chiral LC and

that appealing to both MEF and PBG pathways. Further, we demonstrate that the different systems studied can be electrically switched between two states to modulate the fluorescence. The results bring out the feature that the conjunctive pathway also leads to the highest modulation amplitude. Being generic in nature the protocol employed can be adapted to a variety of situations with the large magnitude as well the modulation level suitable for applications such as biosensors, various analyte detection, and other photonic devices.

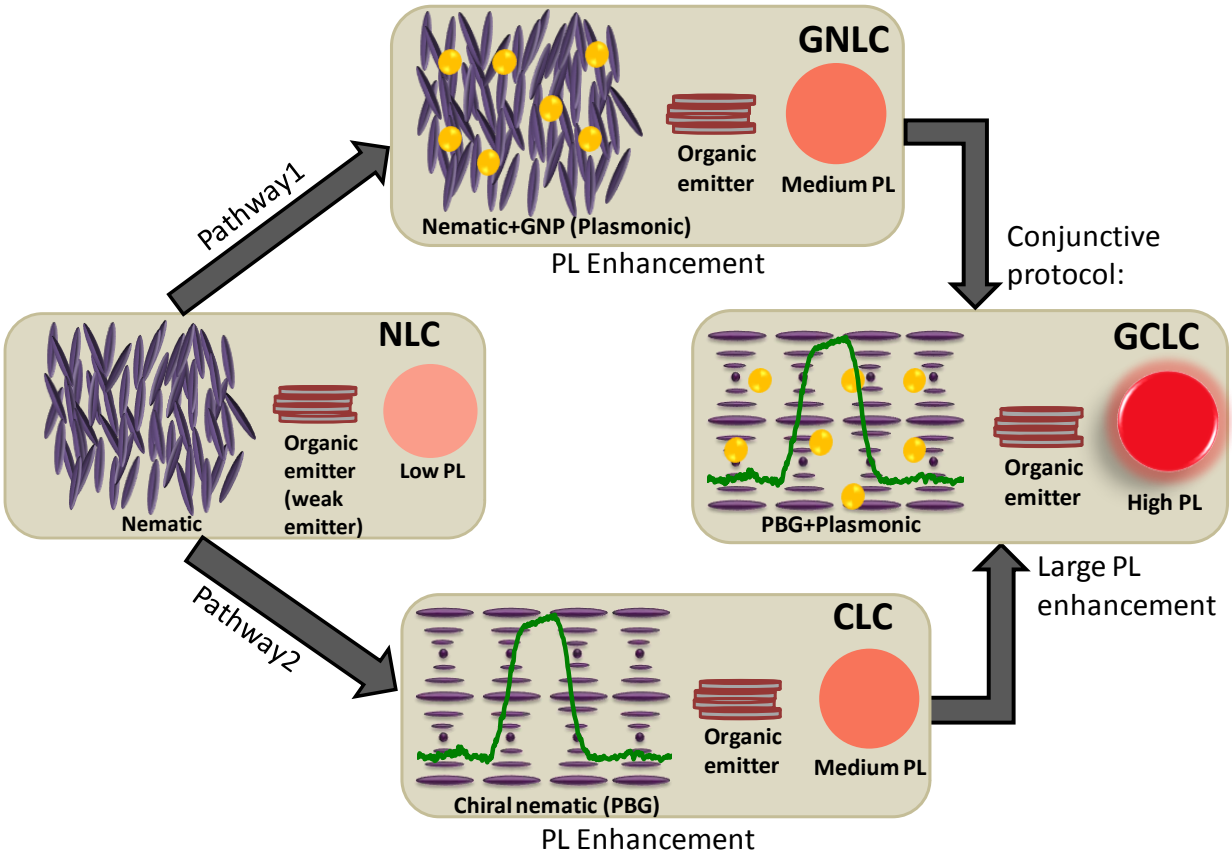

Figure 7: Schematic illustration of the conjunctive protocol for photoluminescence enhancement. The two independent pathways, viz., plasmonic (Pathway 1, material GNLC)) and PBG (Pathway 2, material CLC) yield comparable emission levels, each of which being higher than that for the simple case of NLC having just the nematic and the organic emitter . In contrast, the conjunctive protocol (material GCLC) having contributions from both PBG and plasmonic aspects leads to PL level which is much larger than the sum of the two individual contributions. The violet ellipses represent the LC molecules, the yellow spheres, the gold nanoparticles and the brown discs, the organic emitter molecules. The green peak shown in the CLC and GCLC panels suggests the PBG optical absorption feature of the underlying helical organization of the LC molecules. The PL level for each situation is indicated by red circular discs in each panel, with its intensity, a measure of the emission magnitude.

Chapter 7: Confinement of an antiferroelectric liquid crystal in a polymer nanonetwork: Thermal and dielectric behavior

In this chapter, thermal and dielectric investigations on a liquid crystal exhibiting an antiferroelectric phase is confined in a polymer network of sub-micron dimensions are described. Introducing one dimensional periodicity over the orientational order, one realizes layered smectic phases: Smectic A (SmA), if the director is along the layer normal and smectic C (SmC), if it is at an angle. If the molecules are chiral, a precession of the in-plane **c** director occurs between successive layers, resulting in a macroscopic helix. A more important consequence of the chirality is the lowering of the symmetry of the structure that leads to the appearance of ferroelectricity in the chiral SmC (SmC*) phase [24]. In a variant of this phase, known as the antiferroectric SmC* or SmCA* phase, the **c** director points in almost opposite directions to the neighbouring layers [25]. This causes the polarization direction to alternate between the layers. There are various relaxation modes associated with these diffrent smectic phases. The molecular processes correspond to the independent motions of the individual molecules, where as the collective process arise from their cooperative motion. The dielectric parameters of these modes, such as the strength and relaxation frequency can be related to properties like polarization, pitch, tilt angle etc. These collective relaxation modes are referred to as the Soft mode (occurring in the 10^3 - 10^6 Hz range) and the Goldstone mode (10 – 10^3 Hz range). While both the modes are present in the SmC* phase only the soft mode is observed in the SmA phase. SmC_A* phase has many interesting properties such as the tristate switching and double hysteresis loop in the polarization-electric (P-E) field. The chapter describes thermal and dielectric behavior in the SmC_A^* and SmA phases of a material confined in a polymer matrix. Two different photopolymerizable monomers have been employed for the purpose: one of them (HDDA) is bereft of any aromatic parts, while the other (RM82) contains aromatic as well as aliphatic units and, in fact, exhibits a liquid crystalline phase in its monomeric state. The polymerization, which is carried out in the presence of the liquid crystalline host, is expected to yield a nano segregated structure for HDDA and blended structure for the RM82 case, the difference reflecting in the morphologies of the networks, as evidenced by SEM images. Surprisingly, even a small concentration of the latter polymer added to the former variety has substantial influence on the morphology. The main work focuses on calorimetry and dielectric relaxation spectroscopy of the

host liquid crystal confined in these nanonetworks created by the polymers, which can be considered to form virtual surfaces with a finite anchoring energy. We have investigated the in-phase and antiphase modes in the antiferroelectric phase, and the soft mode in the paraelectric phase preceding the antiferroelectric phase. The relaxation frequency of all these modes is substantially influenced by the network, with the results showing certain surprises in cases containing both HDDA and RM82.

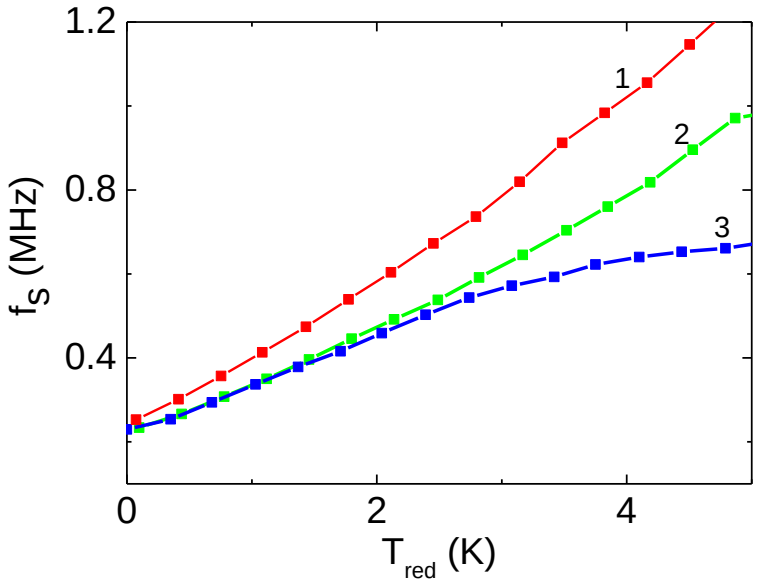

Figure 8: Temperature dependence (T_{red} = $T–T_c$) of the soft mode relaxation frequency for (1) TFM, (2) TFM10HD and (3) TFM9HD1RM samples.

Figures 8 presents the temperature dependence of f_s, the relaxation frequency of the soft mode for TFM and the two PN samples, TFM10HD and TFM9HD1RM having 10% HDDA, and 9% HDDA +1% RM82, respectively. The overall behaviour in all the cases is as expected which is f_s increases as $T–T_c$ increases, i.e. on moving away from the SmA-SmC_A^* transition (here T_c is the SmA-SmC_A^* transition temperature. However, the former two exhibit a continuous increasing frequency, while TFM9HD1RM has a limiting behaviour on moving away from the transition T_c. The interesting feature to be noted here is that the presence of the polymer network lowers the relaxation frequency suggesting that the hindrance to the associated tilt fluctuations is increased when the sample is confined in the polymer network.

Chapter 8: Outlook and future prospective

This section provides a comprehensive overview of the work described above with their potential applications and the future outlook.

References

1. S. Chandrasekhar, Liquid crystals, Cambridge University Press, 2nd edition (1994).
2. P. G. de Gennes and J. Prost, The Physics of Liquid Crystals, Oxford Science Publication, Oxford (1993).
3. See for example Liquid Crystal Displays, Fundamentals Physics and Technology, R.H. Chen (John A Wiley and Sons), 2011.
4. D.Scutaru, I.Carlescu, E.R.Bulai, C.I.Ciobanu, G.Lisa, N.Hurduc, Bent-Core Liquid Crystals: Structures and Mesomorphic Properties. IntechOpen Limited, United Kingdom 2018
5. H. M. J. Boots, J. G. Kloosterboer; C. Serbutoviez, and; Touwslager, F. J. Polymerization-Induced Phase Separation. 1. Conversion−Phase Diagrams. *Macromolecules* **29**, 7683 (1996)
6. C. Serbutoviez, J. G. Kloosterboer, H. M. J. Boots, F. J. Touwslager, Polymerization-Induced Phase Separation. 2. Morphology of Polymer-Dispersed Liquid Crystal Thin Films. *Macromolecules* **29**, 7690 (1996)
7. I. Dierking, Recent Developments in Polymer Stabilised Liquid Crystals. *Polym. Chem*. **1**, 1153, (2010).
8. D.Broer, G. P. Crawford, S.Zumer, G. P. Crawford, S. Zumer, Cross-Linked Liquid Crystalline Systems; Broer, D., Crawford, G. P., Zumer, S., Eds.; CRC Press, 2011.
9. P. L.Madhuri, S.K. Prasad, G. G. Nair, Influence of Polymer Stabilization on the Dielectric Relaxations of an Antiferroelectric Liquid Crystal. *RSC Adv.*,**4**, 3121 (2014).
10. (10) H.-S. Kwok, S.Naemura, H. L. Ong, Progress in Liquid Crystal Science and Technology : In Honor of Shunsuke Kobayashi's 80th Birthday; World Scientific, 2013.
11. I.Dierking, A Review of Polymer-Stabilized Ferroelectric Liquid Crystals. *Materials* (Basel)., **7**, 3568 (2014).
12. J.Kim, J. I. Han, Effect of Liquid Crystal Concentration on Electro-Optical Properties of Polymer Dispersed Liquid Crystal Lens for Smart Electronic Glasses with Auto-Shading and Auto-Focusing Function. *Electron. Mater. Lett*. **10**, 607 (2014).
13. I. Dierking, Nanoscience with liquid crystals, Liquid Crystals Today, 26, 63-65 (2017)
14. Q. Li (Ed.), Functional Organic and Hybrid Nanostructured Materials: Fabrication, Properties, and Applications, Wiley-VCH, Weinheim, 2017 (ISBN 978-3-527-34254-9)
15. S. P. Yadav, S.Singh, Carbon nanotube dispersion in nematic liquid crystals: An overview; *Progress in Materials Science* **80,** 38 (2016)
16. S. A. Zangana, M.Iliut, M.Turner, A.Vijayaraghavan, I.Dierking, Properties of a Thermotropic Nematic Liquid Crystal Doped with Graphene Oxide; *Adv. Opt. Mater.* **4** , 1541 (2016)

17. K. Abha, J. Nebu, J. S. Anjali Devi, R. S. Aparna, R. R. Anjana, A. O. Aswathy and S. George, Sensors Actuators, B Chem. **282**, 300 (2019).
18. H. Nguyen-Ngoc and C. Tran-Minh, *Anal. Chim. Acta*, **583**, 161 (2007).
19. X. Zhang, N. Y. Xu, Q. Ruan, D. Q. Lu, Y. H. Yang and R. Hu, *RSC Adv*. **8**, 5714 (2018)
20. N. Siraj, B. El-Zahab, S. Hamdan, T. E. Karam, L. H. Haber, M. Li, S. O. Fakayode, S. Das, B. Valle, R. M. Strongin, G. Patonay, H. O. Sintim, G. A. Baker, A. Powe, M. Lowry, J. O. Karolin, C. D. Geddes and I. M. Warner, *Anal. Chem*. **88**, 170 (2016).
21. I. Kim, J.-S. Moon, K. Kyhm and J.-W. Oh, *Mol. Cryst. Liq. Cryst*. **654**, 1 (2017).
22. S. Hu, Y. Ren, Y. Wang, J. Li, J. Qu, L. Liu, H. Ma and Y. Tang, Beilstein *J. Nanotechnology*,**10**, 22 (2010).
23. J. R. Lakowicz, K. Ray, M. Chowdhury, H. Szmacinski, Y. Fu, J. Zhang and K. Nowaczyk, *Analyst*, **133**, 1308 (2008).
24. A.D.L. Chandani., Y. Ouchi, H. Takezoe, A. Fukuda, K. Furukawa and A. Kishi, *Jpn. J. Appl. Phys.* **28**, L1261 (1989)
25. Musevic. I, Blinc. R and Zeks.B , The Physics of Ferroelectric and Antiferroelectric Liquid Crystals (World Scientific, Singapore, 2000)

The following is the list of publications resulting from the work carried out by the candidate and in the order appearing in the text:

1. S.K.Prasad, **M.Baral**, A.Murali, S.N.Jaisankar, 'Carbon Nanotube Reinforced Polymer-Stabilized Liquid Crystal Device: Lowered and Thermally Invariant Threshold with Accelerated Dynamics.' *ACS Appl. Mater. Interfaces.* **9**, 26622 (2017)

2. **M**. **Baral,** K. Bramhaiah, N.S. John, S.K. Prasad,'Graphene-Augmented Polymer Stabilization: Drastically Reduced and Temperature-Independent Threshold and Improved Contrast Liquid Crystal Device.' *ACS Omega*, **4**, 403. (2019)

3. **M.Baral**, S.K.Prasad, H.Patel, A.S.Achalkumar, C.V.Yelamaggad, 'Giant enhancement of photoluminescence and tertiary emission in a chiral nematic by matching photonic band gap and excitation wavelength.' *J. Mol. Liq.* **262**, 354. (2018)

4. **M.Baral,** V,N.Veerabhadraswamy, S.K.Prasad, C.V.Yellamagad, 'Enhanced photoluminescence in a chiral nematic liquid crystal through polymer stabilization and an erasable 3-state memory device.' *J. Mol. Liq.* **292**, 111338 (2019)

5. **M.Baral,** S.K.Prasad, C.V.Yellamagad, S.A.Bhatt; (2019) 'Conjunctive photoluminescence enhancement through plasmonic and photonic band gap pathways in a chiral self-assembled system.' *ChemPhotoChem,* **4**, 582 (2020)

6. **M.Baral**, A.P.Ranjitha, S.K.Prasad, 'Confinement of an antiferroelectric liquid crystal in a polymer nanonetwork: thermal and dielectric behaviour.' *Bulletin of Materials Science,* **41**, 135 (2018)

Details of the patent applications based on the above research work:

1 Polymer stabilized liquid crystal device, composition and method thereof, Patent date: Filed Jan 20, 2017 application no- 201741002313

2 A method of enhancement of photoluminescence in a chiral nematic liquid crystal, Patent date: Filed Jun 12, 2017 application number- 201741020498

Two book chapters resulting from the research work carried out by the candidate:

1. 'Influence of Gulliver over Lilliput: Novel properties of Carbon nanotubes/liquid crystal composites.' Authored by S.K.Prasad, D.S.S.Rao, M.Baral and G.V.Varshini ; Book Title- 'Organized Networks in Carbon Nanotubes' CRC Press/Taylor & Francis Group, USA
2. 'Polymers for confinement of liquid crystals: Influence of inorganic inclusions' Book Title - Liquid Crystal Polymer Nanocomposites, Ed. Visakh. P. M, Artem Semkin, Zeynep Güven Özdemir, Publisher: Elsevier, Oxford, UK (book chapter under preparation)

(MARLIN BARAL)

Forwarded through

Dr.S.Krishna Prasad
(Research Supervisor)

Head of the institution